

Hydrogen analysis depth calibration by CORTEO Monte-Carlo simulation

M. Moser^{a,*}, P. Reichart^a, A. Bergmaier^a, C. Greubel^a, F. Schiettekatte^b,
G. Dollinger^a

^a*Universität der Bundeswehr München, Institut für Angewandte Physik und Messtechnik
LRT2, Fakultät für Luft- und Raumfahrttechnik, 85577 Neubiberg, Germany*

^b*Université de Montréal, Département de Physique, Montréal, QC, Canada H3C 3J7*

Abstract

Proton-proton (pp) scattering has proven to be the most sensitive ion beam method for hydrogen analysis [1] due to the unique signature of the two protons emitting from the point of scattering with 90° angle to each other. Provided that the proton energy is large enough, a huge solid angle of detection of few sr can be used in transmission geometry and hence, for microscopic hydrogen imaging in 3 dimensions it is in fact the only method because of its low radiation damage potential [2]. For proton energies below 5 MeV the sample thickness is limited to few microns. At the nuclear microprobe SNAKE up to 25 MeV are possible and samples of more than 100 μm thickness can be investigated.

Depth information is evaluated from the energy sum signal with respect to energy loss of both protons on their path through the sample. In first order, there is no angular dependence due to elastic scattering. In second order, a

*Corresponding author

Email addresses: `marcus.moser@unibw.de` (M. Moser),
`guenther.dollinger@unibw.de` (G. Dollinger)

1
2
3
4
5
6
7
8
9 path length effect due to different energy loss on the paths of the protons
10 causes an angular dependence of the energy sum. Therefore, the energy sum
11 signal has to be de-convoluted depending on the matrix composition, i.e.
12 mainly the atomic number Z , in order to get a depth calibrated hydrogen
13 profile. Although the path effect can be calculated analytically in first order,
14 multiple scattering effects lead to significant deviations in the depth profile.
15 Hence, in our new approach, we use the CORTEO Monte-Carlo code [3]
16 in order to calculate the depth of a coincidence event depending on the
17 scattering angle. The code takes individual detector geometry into account.
18 In this paper we show, that the code correctly reproduces measured pp-
19 scattering energy spectra with roughness effects considered. With Mylar-
20 sandwich targets (Si, Fe, Ge) we demonstrate the deconvolution of the energy
21 spectra on our current multistrip detector at SNAKE. As a result, hydrogen
22 profiles can be evaluated with an accuracy in depth of about 1% of the
23 sample thickness.
24
25
26
27
28
29
30
31
32
33
34
35
36

37 *Keywords:*

38 proton-proton scattering, hydrogen analysis, hydrogen depth profiling,
39 monte-carlo simulation, multiple scattering, multi strip detector
40
41
42
43
44
45
46
47
48
49
50
51
52
53
54
55
56
57
58
59
60
61
62
63
64
65

1
2
3
4
5
6
7
8
9 **1. INTRODUCTION**

10
11
12 For quantitative detection of hydrogen by coincident elastic proton-proton
13 (pp) scattering has to be proven as one of the most sensitive methods with a
14 detection limit in the sub-ppm range [1]. Due to the lowest damage potential
15 of all ion beam probe methods for hydrogen analysis [2], this method is
16 the only one to analyze hydrogen distributions with μm resolution by using
17 proton microprobe imaging [4]. The scattering analysis has to be performed
18 in transmission geometry (Fig. 1a) so that the scattered protons can be
19 detected in coincidence with an angular sum of 90° to each other as a unique
20 signature. At SNAKE we use two pairs of matrix structured detector to look
21 for this pattern as described in [5]. Due to the energy loss which is described
22 by the stopping power $S = dE/dz$ for protons, the depth of the detected
23 hydrogen atom scattered from the sample is correlated to the energy sum
24 $E_{\text{sum}} = E_1 + E_2$ of the two scattered protons from each event. Thus a depth
25 distribution of about 5–10 % of the total thickness is obtained, this usually
26 corresponds to few μm resolution, even sub- μm resolution is possible for
27 lower energies.

28
29 The de-convolution of the energy sum signal to a depth value is a non-
30 trivial task because the energy signal from equal depths is affected by the
31 path length effect and hence depends on the scattering angle or the energy
32 difference. This causes bending of the depth lines as visible in Fig. 1b and is
33 described in detail in [2]. It has to be addressed in particular for transmission
34 geometry, where we use huge solid angle of detection of about 2 sr in order to
35 get the optimum ratio of signal to damage events [2]. Up to now we solved
36 this deconvolution by a first order approximation: The energy sum signal
37
38
39
40
41
42
43
44
45
46
47
48
49
50
51
52
53
54
55
56
57
58
59
60
61
62
63
64
65

1
2
3
4
5
6
7
8
9
10 26 from front and back surface is extracted for each scattering angle/energy dif-
11 27 ference value and the depth is approximated by linear decrease from front and
12
13 28 back surface value. Even for low hydrogen content the surface signal is clearly
14
15 29 visible due to natural surface contamination, otherwise it can be prepared
16
17 30 by adding Mylar to front and back. However, of course this approximation
18
19 31 adds uncertainties to a quantitative evaluation of the depth profiles.

20
21 32 In our new approach we use the CORTEO code as a very fast Monte-
22
23 33 Carlo-Simulation [3]. The simulation includes all geometric properties of the
24
25 34 individual detection setup as it has been used before similarly in the case
26
27 35 of coincident carbon-carbon scattering [6]. With this we simulate a spectra
28
29 36 for the requested matrix composition with a defined homogeneous depth
30
31 37 distribution of hydrogen. The output parameters of the scattering events
32
33 38 are fed into the coincidence analysis like measured data with the same filter
34
35 39 settings of the coincidence analysis. The point of origin of the scattering event
36
37 40 is known from the simulation code and is then assigned by a fitting routine
38
39 41 to the energy sum for each scattering angle. This gives the de-convoluted
40
41 42 energy signal as a calibrated depth profile. Additionally, with the inclusion
42
43 43 of all coincidence filters, we are also able to calibrate the depth dependent
44
45 44 efficiency of the filters caused by multiple scattering effects. This will be
46
47 45 addressed in a forthcoming paper.

48
49 46 In Section 2 we will at first proof that the generated energy signal from the
50
51 47 code is in agreement with the measured data as well as analytical functions
52
53 48 for energy loss and energy spread. Later we will describe the deconvolution
54
55 49 of the energy spectra to gain depth profiles and give some examples using
56
57 50 our current pp-detector setup.

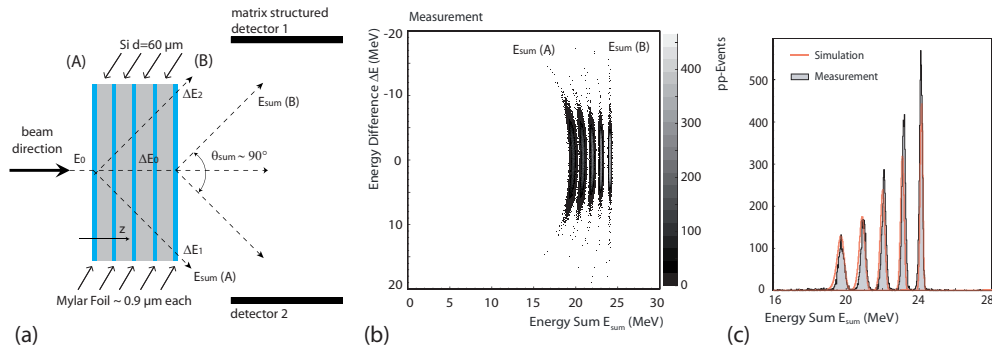


Figure 1: (a) Principle of the scattering geometry for coincident pp-scattering analysis with a position sensitive detector system. Furthermore, the sample exists of four $(60 \pm 10) \mu\text{m}$ thick Si-wafer in a sandwich configuration of 900 nm thick Mylar layers in order to get a clear hydrogen signal with defined hydrogen content $(3 \times 10^{18} \text{H} - \text{at}/\text{cm}^2)$ each as illustrated. (b) The measured energy sum E_{sum} in dependence on the energy difference ΔE of the both detected protons for the sample (see (a)), incident proton energy of $E_0 = 25 \text{ MeV}$. (c) Projection of the pp-events onto the energy sum axis compared with the CORTEO simulation (red line).

2. SIMULATION OF ENERGY SPECTRA

Experimental setup

In a first study we used a simple pp-detector setup in order to compare the simulated CORTEO energy spectra with experimental data. As illustrated in Fig. 1a, the setup consists of two $1000 \mu\text{m}$ thick Silicon detectors with 7 horizontal strips each (Micron semiconductor Design I) covering a solid angle of detection of $\Delta\Omega \approx 2.65 \text{ msr}$. The energy resolution was determined by elastic scattering on a single Mylar foil with a incident proton energy of 25 MeV to $\delta E_\sigma/E \approx 0.17\%$ for each proton of about 12.5 MeV and each detector side, i.e. $\delta E_\sigma = 20 \text{ keV}$ (1σ width) or $\delta E_{\text{FWHM}} = 50 \text{ keV}$ (FWHM

1
2
3
4
5
6
7
8
9
61 width).

10
11 For testing CORTEO we use a sandwich sample of four $60\ \mu\text{m}$ thick one-
12
13 side polished Si-wafers (as received) with $0.9\ \mu\text{m}$ thick Mylar layers in be-
14
15 tween. This gives a clear hydrogen signal with defined hydrogen density
16
17 of $\rho_{\text{H}}dz = 3 \times 10^{18} \text{H-at}/\text{cm}^2$ each. The sandwich construction was pre-
18
19 pared by stacking some $5 \times 10\ \text{mm}$ large fragments. The planarity of the
20
21 wafer is specified better than 1° and the tolerance in thickness was given as
22
23 $d_{\text{Si}} = (60 \pm 10)\ \mu\text{m}$, but found to be better by profilometer measurements.

24
25 The coincidence events are filtered by Mesytec multistrip detector read-
26
27 out electronics [7] within a time window of $2 - 3\ \text{ns}$ in which both protons
28
29 have to hit opposite strips that define a scattering plane. The angular sum
30
31 $\theta_{\text{sum}} = \theta_1 + \theta_2$ is defined simply by the detector itself. Hence, the angu-
32
33 lar filter condition for $\theta_{1,2} = 45^\circ \pm 5^\circ$ is fixed only to an angular sum of
34
35 $\theta_{\text{sum}} = 90^\circ \pm \mathcal{O}(10^\circ)$.

36
37
38
39 *Experimental data*

40
41 In Fig. 1b the energy difference ΔE of each coincident proton pair is
42
43 plotted in dependence of the energy sum E_{sum} . The energy difference ΔE
44
45 gives an additional angle information due to scattering kinematics. Therefore
46
47 Fig. 1b is a depth profile with scattering angle information. The layers of
48
49 hydrogen from Mylar are represented as lines of same depth. These are bend
50
51 due to the mentioned path length effect [8]. Fig. 1c gives the projection
52
53 onto the energy sum axis and can be interpreted as a hydrogen depth profile
54
55 without correction of the path effect. The hydrogen peaks from Mylar are
56
57 broadened at lower energies due to the path effect, but also due to energy
58
59
60
61
62
63
64
65

1
2
3
4
5
6
7
8
9
10 86 spread of the protons on their way through the sample. This is now directly
11 87 compared to the energy data output of the CORTEO simulation (red line).
12
13 88 The simulated yield is normalized to the measured yield.

14
15 89 One can see that the energy resolution δE_{sum} improves with the depth
16 90 z . The integrated peak content of each layer (gray areas) shows a decrease
17
18 91 of the coincident events due to the fact that multiple scattering destroys the
19
20 92 angular signature of "good" events with increased path length z . Correction
21
22 93 of this effect is not the topic of this paper, but we already want to point out
23
24 94 that CORTEO is in total agreement with the data within our specifications
25
26 95 of sample and setup geometry. Now, we use two parameters to evaluate the
27
28 96 quality of the simulation data: The position of the hydrogen layers and the
29
30 97 spreading of the Mylar layers (peak width).
31

32 33 98 *Layer position*

34
35 99 First, we compare the simulated and measured layer position. In order
36
37 100 to eliminate systematic uncertainties, we fit the first and last peak to the
38
39 101 optimum correlation as done in Fit. [1c](#). This compares to a simple thickness
40
41 102 evaluation by energy loss and gives a mean Si thickness of $d_{\text{Si}} = 4 \times 63.5 \mu\text{m}$,
42
43 103 nominal thickness of Mylar assumed. A fit uncertainty of 10 keV has been
44
45 104 determined corresponding to only $0.6 \mu\text{m}$ in thickness. The result is within
46
47 105 the tolerance of the specifications for the Si thickness and wafer planarity
48
49 106 with respect to our beam size diameter of about 0.5 mm. This is probably
50
51 107 also the reason for the layer position of the three peaks in between showing a
52
53 108 significant systematic shift of about 70 keV, corresponding to about $4 \mu\text{m}$. It
54
55 109 doesn't make sense to evaluate the individual layer thickness and its deviation
56
57 110 due to the unknown planarity and unprecise thickness specification. Hence,

1
2
3
4
5
6
7
8
9 we evaluate the spread function δE_{sum} of each layer and its width $\sigma_{\delta E_{\text{sum}}}$ in
10 the following.
11

12
13 *Layer width*
14

15
16 The widths $\sigma_{\delta E_{\text{sum}}}$ of the Mylar layers are caused by the path effect but
17 also of course by the energy spread due to energy loss scattering and multiple
18 scattering effects that increases with path length of the protons in the sample.
19

20
21 In Fig. [2](#) the measured width $\sigma_{\delta E_{\text{sum}}}$ of each Mylar peak (black squares)
22 is plotted in dependence to the energy sum E_{sum} . The simulated width (red
23 stars) shows a good agreement with the measured data (black squares) when
24 we consider a variation for the one-side roughness of $\approx 1 \mu\text{m}$ and and addi-
25 tionally for the non-planarity of the wavers. In the case of CORTEO, the
26 latter morphologic properties cannot be included, therefore we include a to-
27 tal roughness R_{σ} of $2 \times 1 \mu\text{m}$ for each layer. In fact, this is an assumption
28 that is not representing the physical properties, but with this assumption
29 the $\sigma_{\delta E_{\text{sum}}}(E_{\text{sum}})$ shows the best agreement and we get a mean deviation to
30 the measured data of $\text{Res}(\sigma_{\delta E_{\text{sum}}}) = (18 \pm 11) \text{keV}$ (residuum by quadratic
31 subtraction). Assuming a mean stopping power this corresponds to a devi-
32 ation for the depth spread of $(1.1 \pm 0.6) \mu\text{m}$ that can be interpreted as the
33 accuracy for determining a depth resolution.
34
35

36
37 The peak widths are also in agreement with analytical models from energy
38 loss straggling [\[9\]](#) and small angle scattering [\[10\]](#). Taking these contributions
39 on all paths of the protons and also the detector energy resolution as inde-
40 pendent, we get
41
42

$$43 \delta E_{\text{sum}}(E_{\text{sum}}) = \sqrt{2\delta E_{\text{det}}^2 + \delta E_{\text{stragg}}^2(E_{\text{sum}}) + \delta E_{\alpha}^2(E_{\text{sum}}) + \delta E_{\text{path}}^2(E_{\text{sum}})} \quad (1)$$

1
2
3
4
5
6
7
8
9
10
11
12
13
14
15
16
17
18
19
20
21
22
23
24
25
26
27
28
29
30
31
32
33
34
35
36
37
38
39
40
41
42
43
44
45
46
47
48
49
50
51
52
53
54
55
56
57
58
59
60
61
62
63
64
65

134 with δE_{det} being the energy resolution of the detector (1σ), δE_{stragg} the energy
135 loss straggling, δE_{α} the small angle scattering (multiple) path effect and
136 δE_{path} the correlated path length effect as derived in detail in [8].

137 The theoretical model of Eq. (1) is plotted in Fig. 2 (bold black dash
138 line). Additionally for the specified non-planarity of the wavers we add δE_{\parallel}
139 in order to count for a misalignment of each layer that is statistically dis-
140 tributed. This misalignment results in a thickness variation R_{\parallel} similar to a
141 roughness. With this, the theoretical model (bold black dashdot line) is in
142 agreement to the measurement, with $R_{\parallel} = (0.9 \pm 0.1) \mu\text{m}$ where the given
143 uncertainty is drawn as a confidence interval (grey shade). Thus, the modi-
144 fied analytical model show the same agreement as the CORTEO simulation
145 within a mean deviation to the measured data of $\text{Res}(\sigma_{\delta E_{\text{sum}}}) = (20 \pm 3) \text{keV}$.
146 This again corresponds to a spread in depth values of $(1.1 \pm 0.2) \mu\text{m}$. The
147 particular contributions of Eq. (1) are separately plotted (thin black lines)
148 in Fig. 2, showing that energy loss straggling δE_{stragg} in fact gives the major
149 contribution to the total energy spread δE_{sum} .

150 With the agreement of both (Monte-Carlo and analytical) approaches
151 with the experimental data we justify the use of CORTEO to de-convolute
152 the measured energy to a depth scale.

1
2
3
4
5
6
7
8
9
10
11
12
13
14
15
16
17
18
19
20
21
22
23
24
25
26
27
28
29
30
31
32
33
34
35
36
37
38
39
40
41
42
43
44
45
46
47
48
49
50
51
52
53
54
55
56
57
58
59
60
61
62
63
64
65

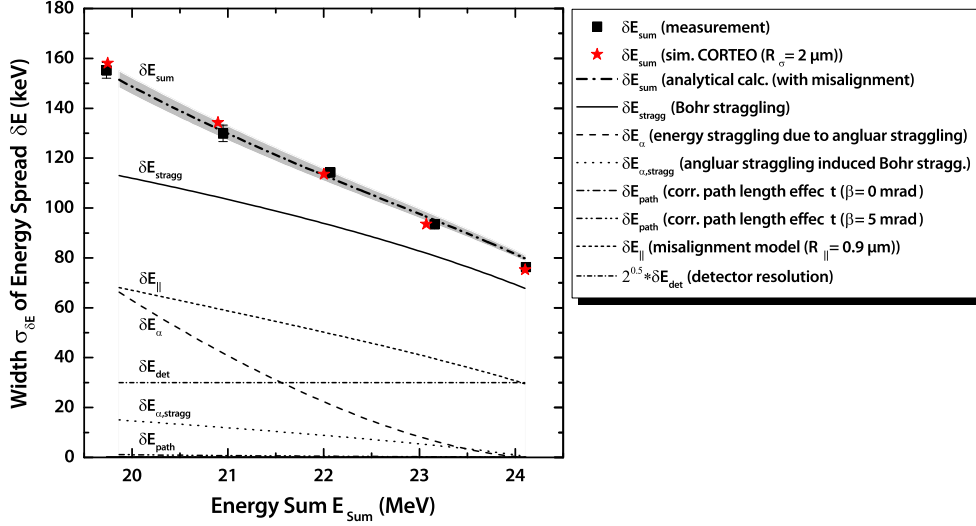


Figure 2: Comparison of the of the energy spread δE_{sum} in dependence on the energy sum E_{sum} . For CORTEO simulation (red stars) and the measured data (black squares) the width $\sigma_{\delta E_{\text{sum}}}(E_{\text{sum}})$ of each Mylar peak is plotted. The results of the simulation with CORTEO (red stars) are plotted with a roughness $R_{\sigma} \sim 2 \mu\text{m}$ of the single sample that counts for the assumed misalignment of the single wavers. The theoretical model (bold black dash line) includes all contributions of Eq. (1) with the separately plotted contributions for the energy spread model δE_{\parallel} that accounts for the thickness variations R_{\parallel} , the detector resolution δE_{det} , the energy loss straggling δE_{stragg} , the small angle scattering path effect δE_{α} and the correlated path length effect δE_{path} . The confidence interval (grey shade) give the uncertainty due to $R_{\parallel} = (0.9 \pm 0.1) \mu\text{m}$.

153 3. DE-CONVOLUTION OF THE ENERGY SPECTRA

154 In the previous section we have shown that the CORTEO code is valid
155 for a quantitative description of the measured coincident pp-events with the
156 depth correlated energy sum E_{sum} . However, the energy sum E_{sum} has to
157 be de-convoluted due to the path length effect for quantitative hydrogen
158 profiles. In the following we demonstrate how to use CORTEO to calculate
159 this de-convolution function using our current pp-detecotr setup.

160 *Experimental setup*

161 The current setup consists of 4 double sided silicon strip detectors (DSSSD,
162 Micron Semiconductor Design W1) with an active area of 50×50 mm and
163 16 strips on each side (back and front). The detectors energy resolution has
164 been determined to $\delta E_{\sigma}/E = 0.23\%$ with $\delta E_{\sigma} = 15$ keV for each proton of
165 about 6.5 MeV and each detector side [11]. The detectors are arranged in a
166 box like structure and each pair of detectors facing each other [11].

167 For a demonstration of the de-convolution procedure we use a similar Si-
168 Mylar-sandwich, but this time we used two, on both side polished Si-wafers
169 with in total three $0.9 \mu\text{m}$ thick Mylar layers. Due to the polishing process,
170 the thickness is reduced to about $56 \mu\text{m}$. In Fig. 3a we show the original
171 energy signal of the coincident pp-events (energy sum E_{sum} vs. energy dif-
172 ference ΔE) using an incident proton energy $E_0 = 13$ MeV. Three lines of
173 pp-events from the Mylar layers are clearly visible. These are separated by
174 the (nominally anhydrous) area of Si-wafers and bent by the path length
175 effect.

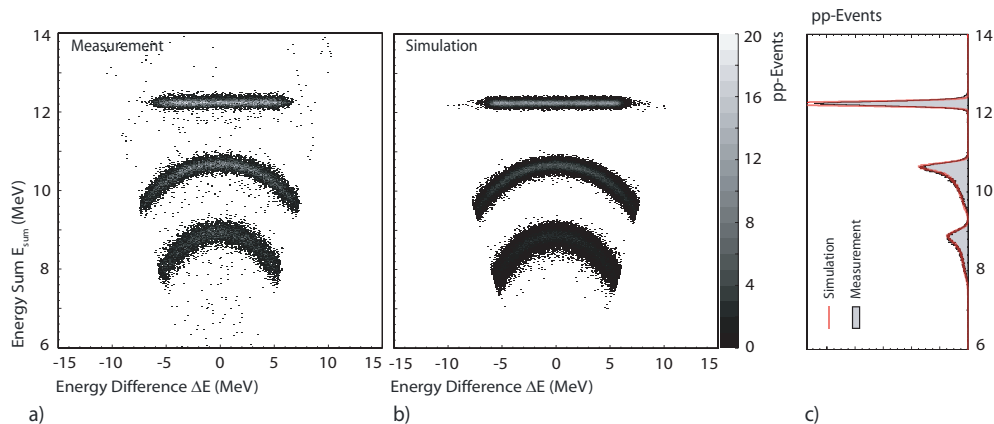


Figure 3: "As received" pp-coincidence spectra of $2 \times 56 \mu\text{m}$ Si-wafer sandwich with $0.9 \mu\text{m}$ Mylar in between and on top (hydrogen content $3 \times 10^{18} \text{ at/cm}^2$ each). (a) Experimental data with current pp-detector setup as described using 13 MeV incident protons. (b) Simulated by CORTEO with same filter conditions and geometry. Note that pixels are filled weighted here due to the applied scattering cross section and give a wrong impression of the content compared to (a). (c) Projection onto energy sum E_{sum} , comparing measurement (black line) and simulation (red line).

176 *Simulation*

177 In Fig. 3b, the energy signal of the same sample configuration but simu-
 178 lated by CORTEO is plotted. Again, the front and back layer is fitted and
 179 we obtain a thickness for Si of $2 \times 55.7 \mu\text{m}$ (fit uncertainty $0.7 \mu\text{m}$). The
 180 simulated pp-events are filtered by the same analysis routine as the exper-
 181 imental data, using the full geometry of the multistrip detection system as
 182 well as its energy and angular resolution. Also, the same dead time corrected
 183 charge Q_{corr} from the experiment was applied to the simulation. CORTEO
 184 uses the pp-scattering cross section data of [12]. Therefore, an equal number
 185 of coincident pp-scattering events appear in the spectrum. This is not visible

1
2
3
4
5
6
7
8
9
10 186 due to weighted filling of the bins from the scattering cross section value,
11 187 but it gets clear in the E_{sum} projection as plotted in Fig. 3c. Also for the
12
13 188 complex structured low energy tails we find a perfect agreement of the both
14
15 189 spectra.

190 *Depth map*

191 The de-convolution function is a mapping of each ΔE - E_{sum} coordinate
192 to a unique depth value. This map is generated by simulating a sample of
193 same composition with a homogeneous hydrogen content and plotting the z -
194 coordinate of the main collision as depth value to the z -axis. This is plotted
195 in Fig. 4 for 115 μm thick silicon. One can see that the depth values of the
196 events are directly correlated with the path length effects. With this map
197 we assign each detected pp-event from the measured $(\Delta E, E_{\text{sum}})_{\text{exp}}$ value a
198 depth z . In detail, we use for this procedure a 2-dimensional fit function in
199 order to assign depth values to events that have energy coordinates outside
200 the simulated spectra.

201 *De-convolution*

202 The result of the applied de-convolution function is demonstrated in Fig.
203 5 with the depth z of each event assigned to the ΔE - E_{sum} coordinate, while
204 ΔE was kept so that $(\Delta E, E_{\text{sum}}) \rightarrow ((\Delta E, z(\Delta E, E_{\text{sum}})))$. The original bent
205 lines representing hydrogen from same layer induced by the path length effect
206 are fully corrected. Fig. 5c shows the corrected spectra with perfect agree-
207 ment of measurement (black line) and simulation (red line). The complex
208 structured low energy tails as shown in Fig. 3c are fully corrected by the

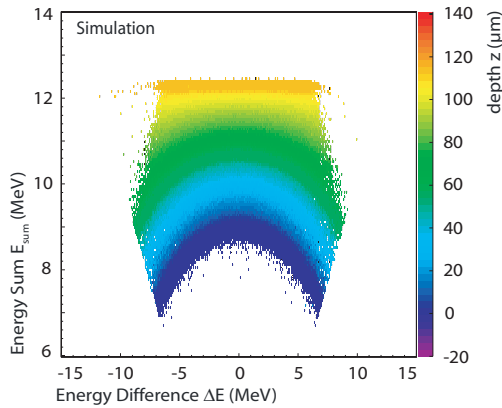


Figure 4: CORTEO simulation of $115 \mu\text{m}$ silicon with a homogeneous hydrogen content. Plotted is the energy sum depending on the energy difference as a function of the depth z of the main collision $(\Delta E, E_{\text{sum}})(z)$ of the both simulated protons for an incident proton energy of 13 MeV .

de-convolution resulting in a homogeneous gaussian distribution of the peak layers.

Heavy materials

At last we show in Fig. 6 that the de-convolution as well as the CORTEO algorithm also works for heavier material in same quality as well as lower proton energies of $E_0 = 13 \text{ MeV}$. Here we used Fe- and Ge-sandwich samples in same way as above. The thickness of the Fe-layers is specified with $(25 \pm 2) \mu\text{m}$ by the manufacturer (Goodfellow) and the simulation of the energy spectra (Fig. 6a) gives agreement with the experimental data as well as the de-convoluted depth profile (Fig. 6b). From simulation we find the Fe-layers in fact to be $24.2 \mu\text{m}$ thick, respectively, with an accuracy for the fit of $0.2 \mu\text{m}$. Hence, we claim a deviation of 3.2% from the nominal value but within the

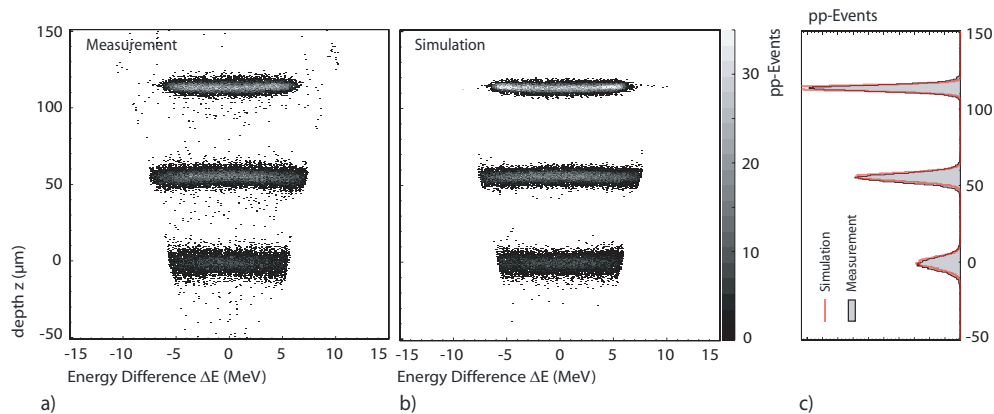


Figure 5: De-convoluted pp-scattering spectra of of the same sample like Fig. 3 using 13 MeV incident protons. The depth z of each event was assigned to the ΔE - E_{sum} coordinate by the de-convolution function, while ΔE was kept so that $(\Delta E, E_{\text{sum}}) \rightarrow ((\Delta E, z(\Delta E, E_{\text{sum}})))$. (a) Experimental data and (b) Simulated data (c) Projection onto depth z , comparing measurement (black line) and simulation (red line).

221 manufacturers specification.

222 In the case of Ge in Fig. 6c and d, we have used polished fragments of a
 223 waver with different thickness around 50 μm . We used this experiment to fit
 224 the unknown thickness by CORTEO simulation and find best agreement
 225 to the experimental data with 57 μm and 46 μm , respectively, with a fit
 226 uncertainty of 0.4 μm . These examples together with the above show for
 227 pp-scattering at energies of 13–25 MeV that determination of layer thickness
 228 by CORTEO fitting is possible even with less than μm -accuracy, although
 229 the depth resolution of the method is limited to few μm .

1
2
3
4
5
6
7
8
9
10
11
12
13
14
15
16
17
18
19
20
21
22
23
24
25
26
27
28
29
30
31
32
33
34
35
36
37
38
39
40
41
42
43
44
45
46
47
48
49
50
51
52
53
54
55
56
57
58
59
60
61
62
63
64
65

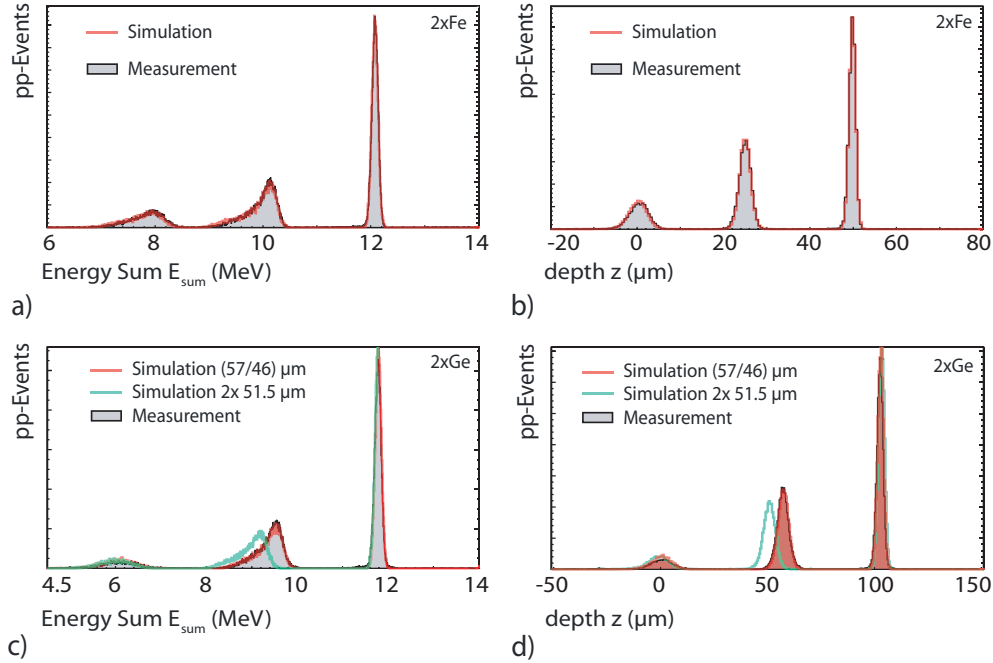


Figure 6: Coincident pp energy sum spectra and (corrected) hydrogen depth profile of 2xFe sandwich sample and 2xGe-sandwich sample with 0.9 μm thick Mylar layers in between and on top. Incident proton energy $E_0 = 13 \text{ MeV}$. (a),(b) For the Fe-sandwich with $(25 \pm 2) \mu\text{m}$ thickness the simulation and measurement are in perfect agreement. (c),(d) The unknown thickness of the polished Ge wavers has been determined by a best fit of the simulated data with 57 μm and 46 μm thickness.

1
2
3
4
5
6
7
8
9
230 **4. CONCLUSION**

231 The energy sum spectra of coincident pp-scattering events corresponds
232 to a hydrogen depth profile. However, this is convoluted by energy spread
233 from energy loss straggling, multiple scattering effects and a strong path
234 length effect, in particular when investigating thick samples or heavier ma-
235 terial. The lower the energy, the better is the depth resolution but also the
236 larger becomes the spread effect. We have shown that CORTEO Monte-
237 Carlo simulation code reproduces the scattering physics very well, so that
238 it can be used to describe material dependent the pp energy spectra. It
239 is also in agreement with analytical description from Bohr straggling and
240 small angle scattering theory. In our demonstration of a Si-sandwich sam-
241 ple, we introduced an additional spread due to misalignment of the sample
242 layers, equivalent to a roughness value. We found that fitting by CORTEO-
243 simulation gives the possibility to evaluate layer spread or roughness with
244 better than μm -accuracy at 13–25 MeV proton energy.

245 The data output of CORTEO can be adapted to the individual detector
246 geometry of a coincidence detector setup and fed into the filter analysis of
247 the data acquisition, giving the same filtered coincidence signal as the exper-
248 imental data. With this, the depth dependent efficiency loss due to loss from
249 multiple scattering effects in the specified angular filter can be simulated and
250 hence corrected for individual matrix compositions. This will be the topic
251 of a forthcoming paper. In this paper we have shown to use CORTEO to
252 generate a de-convolution function to correct the energy spectrum and get
253 a calibrated hydrogen depth profile. With this method, the uncertainty of
254 the depth scale can be reduced to better than 1% of the sample thick-

1
2
3
4
5
6
7
8
9
10
11
12
13
14
15
16
17
18
19
20
21
22
23
24
25
26
27
28
29
30
31
32
33
34
35
36
37
38
39
40
41
42
43
44
45
46
47
48
49
50
51
52
53
54
55
56
57
58
59
60
61
62
63
64
65

255 ness. This is of course a essential requirement for quantification of hydrogen
256 concentration in the depth profile, that is now been solved for any material
257 composition, sample thickness and proton energy combination.

1
2
3
4
5
6
7
8
9
258 **Acknowledgment**

259 The authors are grateful for the financial support provided by the re-
260 search project BMBF-02NUK031A, by DFG project Do938/9 and the Maier-
261 Leibnitz-Laboratorium für Kern- und Teilchenphysik der LMU und TU München.

262 **References**

- 263 [1] P. Reichart, G. Datzmann, A. Hauptner, R. Hertenberger, C. Wild,
264 G. Dollinger, Three-dimensional hydrogen microscopy in diamond, *Sci-*
265 *ence* 306 (2004) 1537.
- 266 [2] P. Reichart, G. Dollinger, A. Bergmaier, G. Datzmann, A. Hauptner,
267 H.-J. Körner, Sensitive 3d hydrogen microscopy by proton proton scat-
268 tering, *Nucl. Instrum. Methods B* 197 (2002) 134.
- 269 [3] F. Schiettekatte, Fast monte carlo for ion beam analysis simulations,
270 *Nucl. Instrum. Methods B* 266 (8) (2008) 1880 – 1885.
- 271 [4] G. Dollinger, P. Reichart, G. Datzmann, A. Hauptner, H.-J. Körner,
272 Three-dimensional hydrogen microscopy using a high-energy proton
273 probe, *Appl. Phys. Lett.* 82 (2003) 148.
- 274 [5] K. Peeper, M. Moser, P. Reichart, E. Markina, M. Mayer, S. Lindig,
275 M. Balden, G. Dollinger, 3d-microscopy of hydrogen in tungsten, *Journal*
276 *of Nuclear Materials* 438, Supplement (0) (2013) S887 – S890.
- 277 [6] I. Bogdanovic-Radovic, M. Jaksic, F. Schiettekatte, Technique for sen-
278 sitive carbon depth profiling in thin samples using c-c elastic scattering,
279 *J. Anal. At. Spectrom.* 24 (2009) 194–198.

1
2
3
4
5
6
7
8
9
10
11
12
13
14
15
16
17
18
19
20
21
22
23
24
25
26
27
28
29
30
31
32
33
34
35
36
37
38
39
40
41
42
43
44
45
46
47
48
49
50
51
52
53
54
55
56
57
58
59
60
61
62
63
64
65

280 [7] MESYTEC GbR, Putzbrunn, Germany, www.mesytec.com.

281 [8] P. Reichart, G. Dollinger, Hydrogen analysis by proton proton scatter-
282 ing, in: Y. Wang, M. Nastasi (Eds.), Handbook of Modern Ion Beam
283 Material Analysis, 2nd Edition, Materials Research Society, 2009.

284 [9] N. Bohr, Mat. Fys. Medd. an. Vid. Selstr. 8 (1948) 18.

285 [10] P. Sigmund, K. B. Winterbon, Small-angle multiple scattering of ions in
286 the screened coulomb region : I. angular distributions, Nucl. Instrum.
287 Methods 119 (1974) 541–557.

288 [11] P. Reichart, C. Greubel, M. Moser, K. Peeper, G. Dollinger, Deuterium
289 microscopy using 17 mev deuteron-deuteron scattering, NIMB these pro-
290 ceedings (**Note to the Editor: Plese reference to this paper that**
291 **will be submitted at IBA2015.**).

292 [12] M. Moser, P. Reichart, C. Greubel, G. Dollinger, Differential protonpro-
293 ton scattering cross section for energies between 1.9 mev and 50 mev,
294 Nucl. Instrum. Methods B 269 (20) (2011) 2217 – 2228.